Determining discharge coefficient of labyrinth and arced labyrinth weirs using support vector machine

Kiyoumars Roushangar, Mohammad Taghi Alami, Jalal Shiri and Mahdi Majedi Asl

ABSTRACT

A labyrinth weir is a linear weir folded in plan-view which increases the crest length and the flow rate for a given channel width and an upstream flow depth. The present study aimed at determining discharge coefficients of labyrinth and arced labyrinth weirs using support vector machine (SVM)-based models. A total of 527 laboratory test data of four types of weirs, namely, Normal and Inverted orientation Labyrinth Weirs in flume (NLW, ILW) and Arced Labyrinth Weirs with and without nappe Breakers in reservoir (ALW, ALWB), were captured from the published literature and utilized to feed the SVM-based models. The obtained results revealed the capability of the SVM-based models in determining discharge coefficients. The results showed that the SVM-based model of arced labyrinth weir (ALW) produced the most accurate results when three dimensionless parameters, e.g. (H_T/P) head water ratio, (α/θ) angle ratio and (L_c/W) magnification ratio, were introduced as input parameters (Root mean square error [RMSE] = 0.013 and R^2 = 0.970 for the test stage). Nonetheless, sensitivity analysis showed that Froude number and head water ratio are the most influential parameters on discharge coefficients of the labyrinth and arced labyrinth weirs, respectively.

Key words | discharge coefficient, labyrinth weirs, nappe breaker, support vector machine (SVM)

Kiyoumars Roushangar (corresponding author)
Mohammad Taghi Alami
Mahdi Majedi Asl
Department of Civil Hydraulic Engineering,
University of Tabriz,
Tabriz,
Iran
E-mail: kroshangar@yahoo.com

Jalal Shiri
Department of Water Engineering, Faculty of
Agriculture,
University of Tabriz,
Tabriz,
Iran

INTRODUCTION

Labyrinth weirs are linear weirs folded in plan-view to increase the crest length for a given canal or spillway width. The flow capacity of a weir is largely influenced by the weir length, L_c, shape of the crest, and the approaching flow conditions (Figure 1). A labyrinth weir can pass large amounts of flow discharge at relatively low heads compared to traditional linear weirs. These weirs are especially well suited for spillway rehabilitation where dam safety concerns, freeboard limitations, and a revised and larger probable maximum flow have required modification or replacement of the spillway (Crookston 2010). As a result, these weirs require less free board than linear weirs, which facilitates flood routing efficiently and allows higher reservoir pool elevations under base-flow conditions (Crookston 2010). Most of the design and performance information on labyrinth

weirs has been developed through physical investigations. Labyrinth weir hydraulics was firstly investigated by Gentilini (1940) when forming triangular weirs by placing a number of oblique weirs together. The development of the modern labyrinth weir design was begun by Taylor (1968) and continued later by Hay & Taylor (1970). In 1985, the Bureau of Reclamation established a design method for engineers to use in the public design and construction of labyrinth weirs (Lux & Hinchcliff 1985). Kocahan & Taylor (2002) discussed that, regardless of the passive control, the labyrinth weir can pass larger amounts of discharge when compared with a regular ogee weir at the beginning of flood events. Crookston & Tullis (2010) compared the hydraulic performance of a normal and inverted orientation labyrinth weir in a channel and found no change in their hydraulic performance.
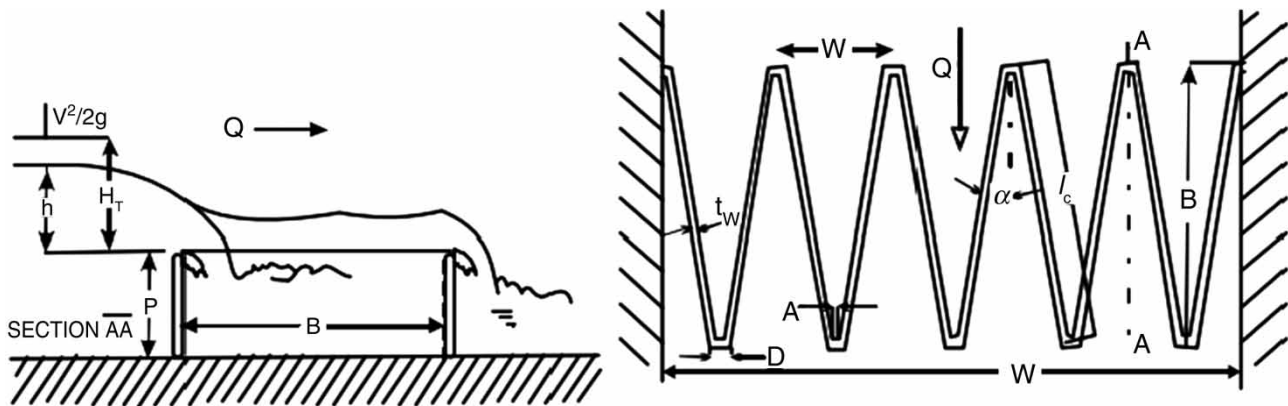
Figure 1 | Plan and elevation views of labyrinth weir.

Christensen (2012) expanded flow characteristics of arced labyrinth weirs. Seamons (2014) developed geometric variation and its effect on efficiency and design method predictions. There is a complex three-dimensional flow over a labyrinth weir, so it is very difficult to find the exact solution of the head-discharge relationship using analytical approaches (Crookston & Tullis 2012).

As an alternative, artificial intelligence-based models may be applied to solve such problems. These techniques have been widely used in recent years as an efficient simulation tool for modeling nonlinear systems and pattern recognition of complex problems. Among others, Bagheri *et al.* (2014) simulated the discharge coefficient of sharp-crested side weirs using artificial neural networks (ANNs). Roushangar *et al.* (2014a) applied ANN and genetic programing (GP) for modeling energy dissipation over stepped spillways. Mohamed & Oliver (2005) developed a discharge equation for a side weir using ANN. Roushangar *et al.* (2014b) developed a GP-based model for river total bed material load discharge. The support vector machine (SVM) technique has been also successfully employed in various water resources engineering issues, including bed load transport prediction (Roushangar & Koosheh 2015), discharge modeling in a compound open channel (Parsaie *et al.* 2015), estimating removal efficiency of settling basins (Singh *et al.* 2008), estimating suspended sediment concentration (Cimen 2008), extrapolation of sediment rating curves (Sivapragasam & Muttil 2005), flood forecasting (Han *et al.* 2007), predicting dissolved oxygen (Li *et al.* 2017), groundwater budget prediction (Gorgij *et al.* 2017) and modeling evapotranspiration (Yin *et al.* 2017). Hanbay *et al.* (2009) applied least square-SVM to predict aeration efficiency on

stepped cascades. Baylar *et al.* (2009) applied least square-SVM in the prediction of aeration performance of plunging over-fall jets from weirs. Azamathulla & Chun Wu (2011) used SVM for computing longitudinal dispersion coefficients in natural streams. Goel (2013) modeled the aeration of sharp crested weirs using SVM. Parsaie & Haghiabi (2014) applied ANN and neuro-fuzzy models to estimate the side weir discharge coefficient. Azamathulla *et al.* (2016) used the SVM technique to determine the discharge coefficient of a side weir. All of the mentioned research confirmed the SVM capabilities in the studied issues. It should however be noted that the previously published papers have mainly focused on labyrinth side weir modeling using SVM and other heuristic data driven models. The purpose of this study is to investigate the performance of the SVM technique for determining the discharge coefficient of four types of labyrinth weirs: normal orientation labyrinth weirs (NLW) and inverted orientation labyrinth weirs (ILW), in flume; arced labyrinth weirs without nappe breakers (ALW) and arced labyrinth weirs with nappe breakers (ALWB), in reservoir. The literature review by the authors showed that such comprehensive SVM-based comparison between labyrinth and arced labyrinth weirs in canals and reservoirs has not been carried out in the existing literature.

MATERIALS AND METHODS

Dimensional analysis

The discharge capacity of a weir refers to the flow rate which can pass over it under a given upstream head. In

this study, a common form of the weirs governing state (Equation 1) was used to quantify the labyrinth weir head-discharge relationship (Henderson 1966).

$$Q = \frac{2}{3} C_d \sqrt{2g} L_c H_T^{3/2} \tag{1}$$

where L_c represents the weir crest length, g denotes the gravitational acceleration, H_T stands for the total head ($H_T = h + v^2/2\,g$), and C_d is the dimensionless discharge coefficient (which represents the weir per-unit length discharge efficiency). This coefficient is an indicator of weir unit width discharge, referred to as hydraulic efficiency, for difference configurations.

C_d might be considered as a function of the total head (H_T), gravitational acceleration (g), dynamic viscosity of the fluid (μ), mass density of the fluid (ρ), surface tension (δ), number of cycles (N), length of weir crest (L_c), cycle sidewall angles (α), cycle arced angle (θ), weir thickness (t_w), length of apex geometry (A), total width of weir (W), width of a single cycle (w), weir height (P), velocity (V), and crest shape (sc) as:

$$C_d = f(v, g, \mu, \rho, \delta, H_T, L_c, W, w, \alpha, \theta, A, N, P, t_w, sc) \tag{2}$$

Dimensional analysis may reduce the dimensions of the input matrix, so would create a low-dimensions space where the number of the studied parameters is low. In this study, C_d can be expressed as a function of dimensionless parameters as:

$$C_d = f(Fr, Re, We, H_T/P, \alpha/\theta, L_c/W, A/w, w/p, t_w/p, sc) \tag{3}$$

where Fr, Re and We are Froude number, Reynolds number and Weber number, respectively.

The American Society of Civil Engineers (ASCE 2000) committee (Manual 97) states that the effects of surface tension on spillways are negligible for $We \geq 100$. The effect of viscosity in a fully turbulent flow is also very small, so the effect of Reynolds number will be eliminated in Equation (3) (Henderson 1966). Nonetheless, weir thicknesses and crest shapes were constant for all the tests. Therefore, Equation (3) is reduced to:

$$C_d = f(Fr, H_T/P, \alpha/\theta, L_c/W, A/w, w/p) \tag{4}$$

Experimental data

Laboratory test data used in this study were those performed by Christensen (2012) and Seamons (2014) at the Utah Water Research Laboratory (UWRL) at Utah State University Campus in Logan. The existing data consist of two experimental sets:

1. Experiments on arced labyrinth weirs and reservoir simulation were conducted in an elevated head box (7.3 m long, 6.7 m wide and 1.5 m deep) by Christensen (2012). After passing over the weirs, the flow drops from a 2.3 m height to a collection channel. There was no structure to control tail water depth. Christensen (2012) tested eight arced labyrinth weirs with and without nappe breakers and three non-arced labyrinth weirs. A schematic representation of the studied labyrinth weirs is displayed in Figure 2. A labyrinth weir layout in which the downstream apexes of each cycle follow the arc of a circle is termed as an arced labyrinth weir (Figure 2(b) and 2(d)). Christensen (2012) suggested that the nappe breakers with a triangular cross-section be placed on the downstream apexes with the point oriented into the flow, as
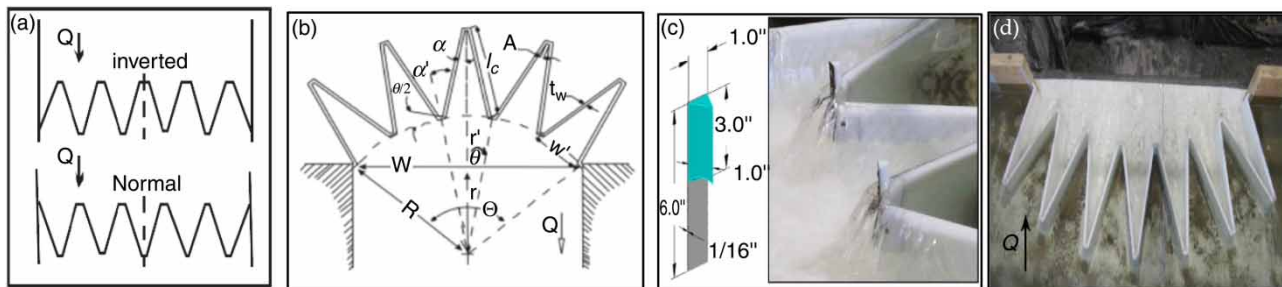

Figure 2 | A labyrinth weir orientation (a), arced labyrinth weir (b) and (d) and labyrinth weir with nappe breakers (c).

shown in Figure 2(c). Nappe breakers vent the nappe to atmospheric pressures, improve stability, and present a potential solution to unstable nappe conditions; however, the decrease in discharge efficiency for arced labyrinth weirs should be accounted for in design. In this part, 227 laboratory test data are used for determining the discharge coefficient of the arced labyrinth weir.

2. Experiments on labyrinth weirs and canal simulation were conducted in a rectangular flume (14.6 m long, 1.2 m wide and 0.9 m deep) by Seamons (2014). For all tests, the slope of the flume floor was set as 0.0 (horizontal). Seamons tested 13 labyrinth weirs and selected 300 laboratory test data (for normal and inverted orientation labyrinth weirs). When the outside apexes of a labyrinth weir attach to the training wall at the upstream or beginning region of the apron, it is termed a 'normal orientation'. The term inverted orientation belongs to the situations where the apexes attach to the training wall at the downstream end of the apron.

Table 1 summarizes the variation range of the parameters used in this study.

Support vector machine

The original SVM algorithm was developed by Vapnik (1995) and the current standard incarnation (soft margin) was suggested by Cortes & Vapnik (1995). SVMs are supervised learning models with associated learning algorithms that analyze data and recognize patterns, and can be used for classification and regression analysis. Whereas the original problem may be stated in a finite dimensional space, the sets to discriminate are not linearly separable in that space. Consequently, it was suggested that the original finite-dimensional space be mapped into a much higher-dimensional space, probably making the separation easier in that space. To maintain a reasonable computational load, the mappings used by SVM schemes are designed to ensure that dot products may be computed easily in terms of the parameters in the original space, by describing them in terms of a kernel function K (x, y) selected to suit the problem. The hyperplanes in the higher-dimensional space are defined as the set of points whose dot product with a vector in that space is constant. The vectors defining the hyperplanes can be elected to be linear combinations with parameters α_i of images of feature vectors that occur in the data base. With this election of a hyperplane, the points in the feature space that are mapped into the hyperplane are defined by the relation: $\sum_{i=1} \alpha_i k(x_i, x) =$ constant, note that if k (x, y) becomes small as y grows further away from x, each element in the sum measures the degree of nearness of the test point x to the corresponding data base point x_i. In this way, the sum of kernels above can be used to measure the relative nearness of each test point to the data points x originating in one or the other of the sets to be discriminated. Different types of kernels are presented in Table 2. General information on the SVM model can be found in, for example, Vapnik (1998).

Table 1 | Variation range of parameters in this study

		NLW and ILW			ALW and ALWB		
	Parameters	**Min**	**Max**	**Values of parameters**	**Min**	**Max**	**Values**
1	Q(cfs)	0.7	22.5	–	0.984	22.059	–
2	H_T/P	0.051	0.835	–	0.094	0.873	–
3	C_d	0.309	0.684	–	0.409	0.733	–
4	W(in)	–	–	48.41, 45.41	72	142.551	–
5	N	–	–	2	–	–	5, 7, 9
6	α(degree)	–	–	12,15	–	–	12, 20
7	θ(degree)	–	–	–	–	–	10, 20, 30
8	t_w(in)	–	–	1.45	–	–	1
9	P(ft)	–	–	1, 1.25, 1,5	–	–	0.666
10	L_c(in)	98.5	214.1	–	203.5	634	–

Table 2 │ Different kernel functions

Function	Expression
Linear	$K(x_i, x_j) = (x_i, x_j)$
Polynomial	$K(x_i, x_j) = ((x_i, x_j) + 1)^d$
Radial basis function	$K(x_i, x_j) = \exp\left(-\dfrac{\|x_i - x_j\|^2}{2\sigma^2}\right)$
Sigmoid	$K(x_i, x_j) = \tanh(-\alpha(x_i, x_j) + c)$

Study protocol and models evaluation

Figure 3 illustrates the schematic representation of the study flowchart. Ten different input combinations for normal and inverted orientation labyrinth weirs (NLW, ILW) and eight different input combinations for arced labyrinth weirs with and without nappe breakers (ALW, ALWB) were examined in the present study (see Table 3). Experimental data were divided into training and testing parts: 75% of the whole data were used for training (establishing) the models and the remaining data (25% of the whole data) were used for testing, randomly. The performances of the SVM models were evaluated by the root mean square error (*RMSE*), Nash and Sutcliffe coefficient (*NS*) and coefficient of determination (R^2) criteria:

$$RMSE = \sqrt{\frac{1}{N}\sum_{i=1}^{N}(C_{d0i} - C_{dpi})^2} \tag{5}$$

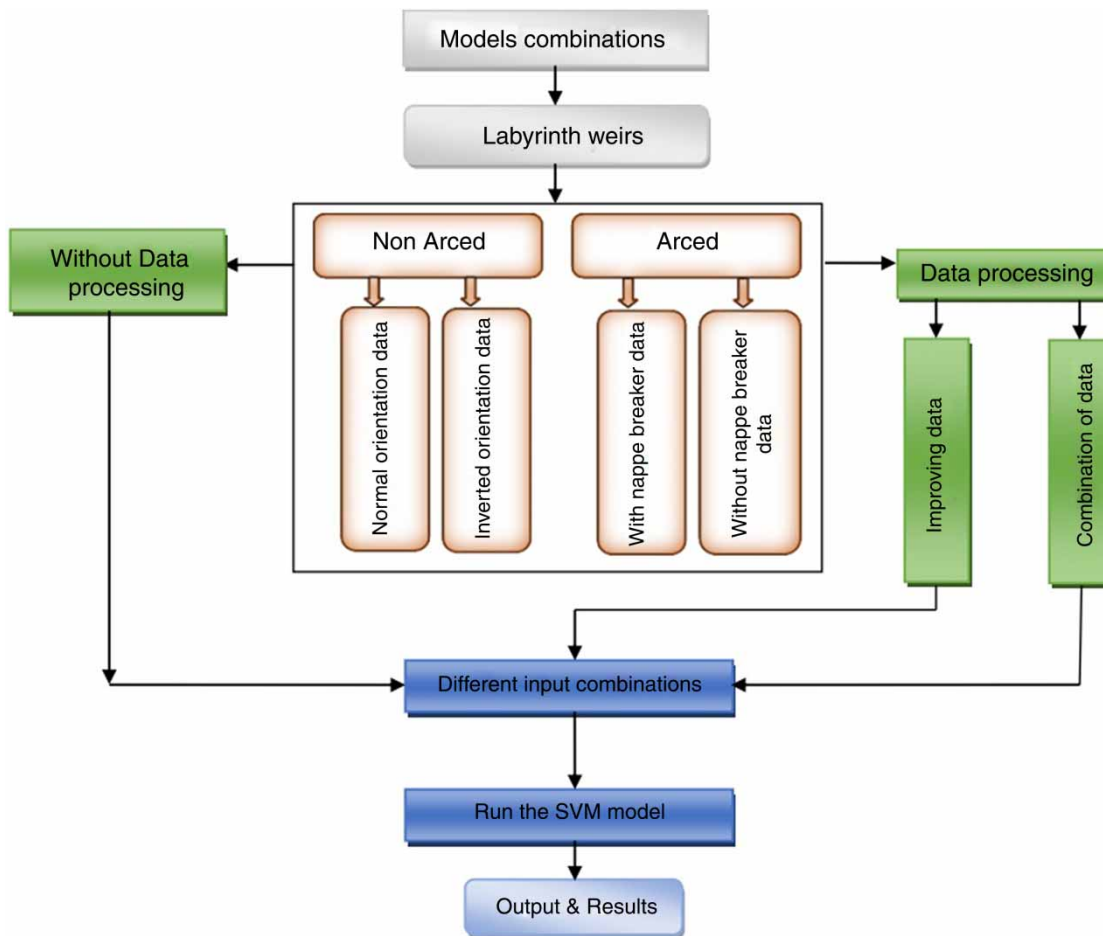$$NS = 1 - \frac{\sum_{i=1}^{N}(C_{d0i} - C_{dpi})^2}{\sum_{i=1}^{N}(C_{d0i} - \bar{C}_{do})^2} \tag{6}$$

Figure 3 │ Schematic representation of the study flowchart.

Table 3 | Different input combinations applied in the present study

Model	Input parameters	Model	Input parameters
Normal and inverted orientation labyrinth weirs (NLW, ILW)			
Model 1	H_T/P	Model 6	$H_T/P, L_c/W, A/w$
Model 2	$H_T/P, \alpha$	Model 7	$H_T/P, \alpha, w/p$
Model 3	$H_T/P, \alpha, A/w$	Model 8	$H_T/P, L_c/W$
Model 4	$H_T/P, \alpha, L_c/W, A/w$	Model 9	$H_T/P, \alpha, L_c/W, A/w, w/p, Fr$
Model 5	$H_T/P, \alpha, L_c/W, A/w, w/p$	Model 10	$H_T/P, L_c/W, A/w, Fr$
Arced labyrinth weirs with and without nappe breakers (ALW, ALWB)			
Model 1	H_T/P	Model 5	$H_T/P, \alpha/\theta, N, L_c/W, P/t_w$
Model 2	$H_T/P, \alpha/\theta$	Model 6	$H_T/P, N, \alpha/\theta, P/t_w$
Model 3	$H_T/P, \alpha/\theta, N$	Model 7	$H_T/P, L_c/W, \alpha/\theta$
Model 4	$H_T/P, \alpha/\theta, N, L_c/W$	Model 8	$H_T/P, L_c/W$

$$R^2 = \left[\frac{\sum_{i=1}^{N}(C_{doi} - \bar{C}_{do}) \sum_{i=1}^{N}(C_{dpi} - \bar{C}_{dp})}{\sqrt{\sum_{i=1}^{N}(C_{doi} - \bar{C}_{do})^2 \sum_{i=1}^{N}(C_{dpi} - \bar{C}_{dp})^2}} \right]^2 \qquad (7)$$

where C_{d0i} and C_{dpi} denote the observed and corresponding simulated discharge coefficient values at the i-th pattern, respectively. $\bar{C}_{do}$ and $\bar{C}_{dp}$ stand for the mean values of the observed and simulated discharge coefficient values, respectively. N is the number of data patterns.

RESULTS AND DISCUSSION

The present study aimed at evaluating the SVM-based models for determination of the discharge coefficient of normal and inverted orientation labyrinth weirs in flume (NLW, ILW) and arced labyrinth weirs with and without nappe breakers in reservoir (ALW, ALWB). Table 4 shows the results of the sensitivity analysis for SVM model parameters. Figure 4 illustrates the RMSE and R^2 values of various Gamma values of

Table 4 | Sensitivity analysis of SVM model parameters (for ALWB7)

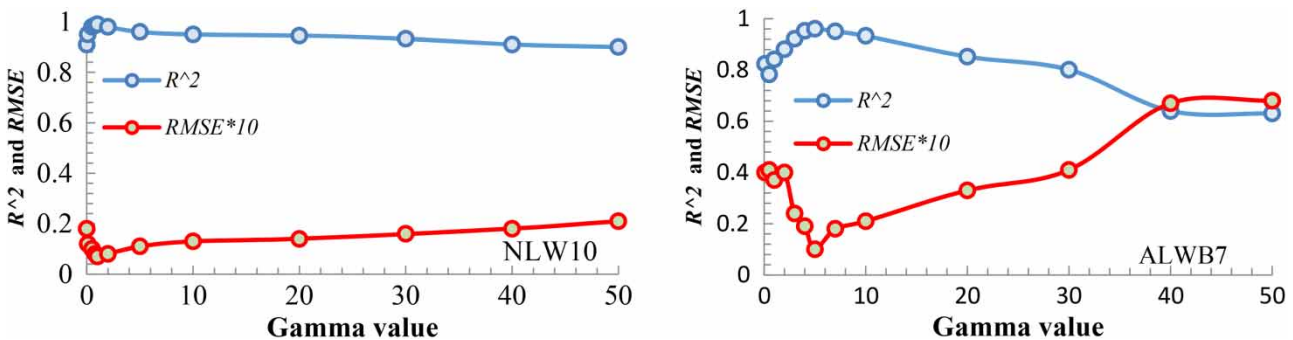| Kernel	R_{Train}	R_{Test}	γ	R_{Train}	R_{Test}	ε	R_{Train}	R_{Test}	C	R_{Train}	R_{Test}
RBF	**0.991**	**0.980**	0.1	0.944	0.943	1	0.285	0.238	1	0.902	0.836
Polynomial	0.916	0.911	1.0	0.960	0.949	0.1	0.981	0.977	10	**0.981**	**0.977**
Linear	0.834	0.807	5.0	**0.981**	**0.977**	0.01	**0.991**	**0.980**	50	0.981	0.977
Sigmoid	0.854	0.831	10	0.986	0.975	0.001	0.991	0.977	100	0.981	0.977
–	–	–	20	0.982	0.851	–	–	–	1000	0.981	0.977

Figure 4 | Variation of RMSE and R^2 vs. Gamma values for NLW10, ALWB7 input configurations.

Table 5 │ The statistical parameters and optimal parameters of SVM model

| Model	Train			Test			c	ε	γ
	R^2	DC	RMSE	R^2	DC	RMSE			
Normal labyrinth weirs (NLW)									
NLW 1	0.863	0.860	0.030	0.846	0.816	0.031	10	0.01	2
NLW 2	0.902	0.898	0.026	0.883	0.869	0.026	10	0.01	4
NLW 3	0.908	0.904	0.025	0.889	0.872	0.026	10	0.01	20
NLW 4	0.972	0.972	0.013	0.956	0.954	0.015	10	0.01	5
NLW 5	0.990	0.979	0.010	0.986	0.979	0.010	10	0.01	12
NLW 6	0.941	0.937	0.023	0.921	0.910	0.020	10	0.01	16
NLW 7	0.992	0.976	0.011	0.986	0.976	0.011	10	0.01	20
NLW 8	0.978	0.975	0.012	0.970	0.969	0.013	10	0.01	20
NLW 9	0.992	0.977	0.011	0.986	0.977	0.011	10	0.01	9
NLW 10	**0.992**	**0.991**	**0.007**	**0.990**	**0.988**	**0.007**	**10**	**0.01**	**1**
Inverted labyrinth weirs (ILW)									
ILW 1	0.900	0.897	0.034	0.868	0.860	0.035	10	0.1	2
ILW 2	0.900	0.898	0.035	0.868	0.860	0.036	10	0.1	2
ILW 3	0.925	0.924	0.031	0.878	0.878	0.035	10	0.1	2
ILW 4	0.919	0.919	0.032	0.878	0.874	0.035	10	0.1	0.1
ILW 5	0.946	0.943	0.026	0.915	0.913	0.029	10	0.1	2
ILW 6	0.921	0.916	0.031	0.930	0.840	0.032	10	0.1	0.5
ILW 7	0.948	0.947	0.020	0.912	0.910	0.026	10	0.1	3.0
ILW 8	0.921	0.921	0.031	0.870	0.869	0.036	10	0.1	3
ILW 9	**0.982**	**0.981**	**0.015**	**0.981**	**0.954**	**0.025**	**10**	**0.1**	**0.5**
ILW 10	0.920	0. 916	0.034	0.872	0.871	0.036	10	0.1	0.5
Arced labyrinth weirs Without nappe breakers (ALW)									
ALW 1	0.855	0.853	0.022	0.822	0.803	0.033	100	0.01	4.1
ALW 2	0.960	0.960	0.010	0.952	0.943	0.016	100	0.01	4.1
ALW 3	0.964	0.960	0.012	0.944	0.935	0.015	100	0.01	3.5
ALW 4	0.960	0.958	0.011	0.952	0.944	0.016	100	0.01	2.5
ALW 5	0.986	0.985	0.009	0.958	0.954	0.016	100	0.01	2.5
ALW 6	0.966	0.963	0.011	0.964	0.942	0.014	100	0.01	2.7
ALW 7	**0.994**	**0.993**	**0.006**	**0.970**	**0.967**	**0.013**	**100**	**0.01**	**4.1**
ALW 8	0.944	0.943	0.011	0.942	0.929	0.017	100	0.01	4.1
Arced labyrinth weirs With nappe breakers (ALWB)									
ALWB 1	0.749	0.748	0.034	0.746	0.713	0.036	10	0.01	1
ALWB 2	0.929	0.928	0.032	0.915	0.913	0.033	10	0.01	5
ALWB 3	0.952	0.951	0.035	0.833	0.813	0.037	10	0.01	1.2
ALWB 4	0.968	0.961	0.030	0.866	0.852	0.032	10	0.01	3
ALWB 5	0.972	0.970	0.008	0.925	0.886	0.014	10	0.01	2.5
ALWB 6	0.974	0.971	0.030	0.868	0.859	0.031	10	0.01	4
ALWB 7	**0.982**	**0.981**	**0.006**	**0.960**	**0.958**	**0.010**	**10**	**0.01**	**5**
ALWB 8	0.835	0.550	0.034	0.831	0.511	0.040	10	0.01	10
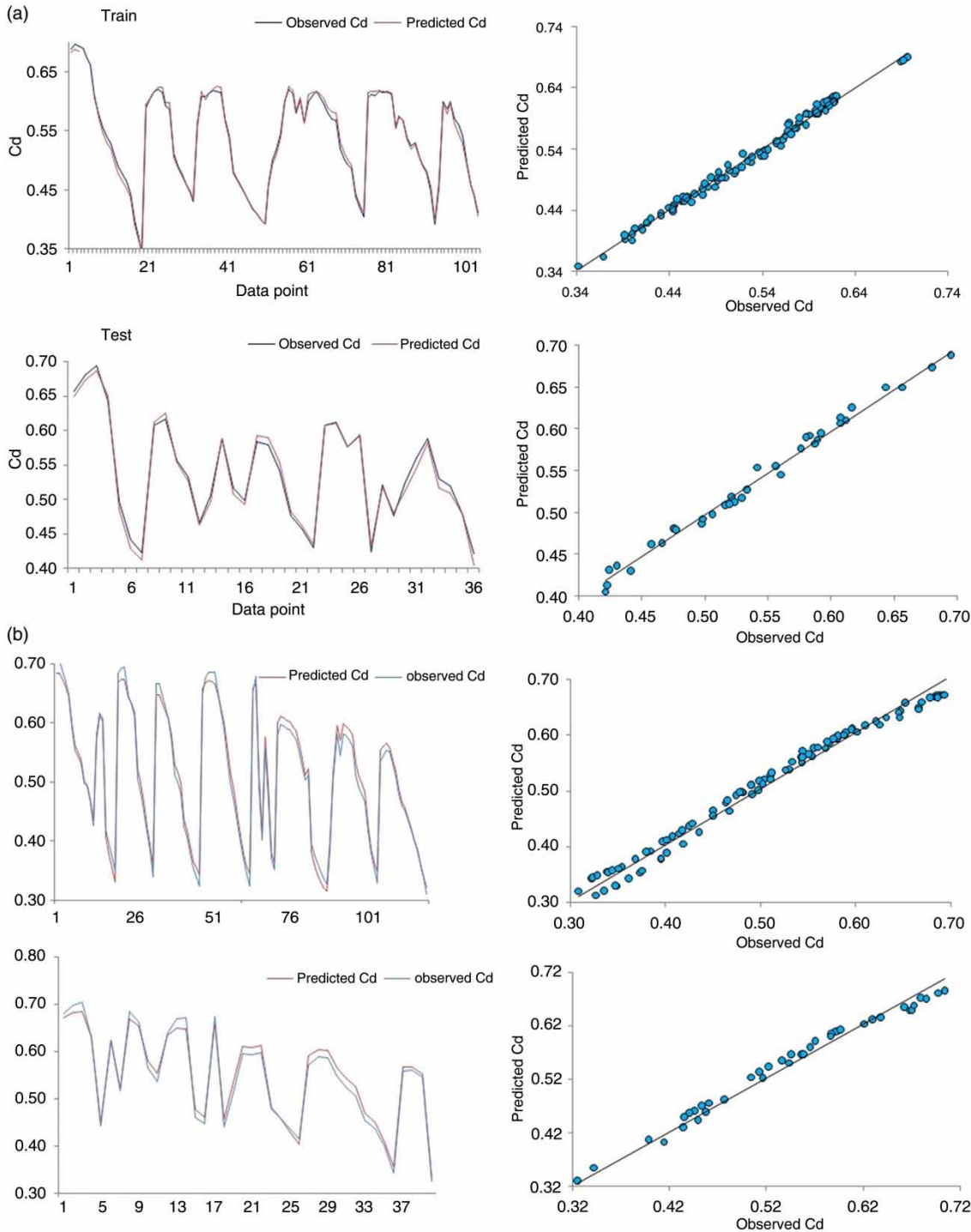
Figure 5 | Comparison of the observed and simulated discharge coefficient values for: (a) Normal labyrinth weir (input configuration 10), (b) inverted labyrinth weir (input configuration 9).

the SVM model (fed with the NLW10 and ALWB7 input configurations). From the figure it is seen that the error statistics fluctuate with changing the Gamma values and the lowest

$RMSE$ and highest R^2 values are obtained when the Gamma values are chosen as 1 and 5 for the NLW10 and ALWB7 input combinations, respectively. Very small Gamma values
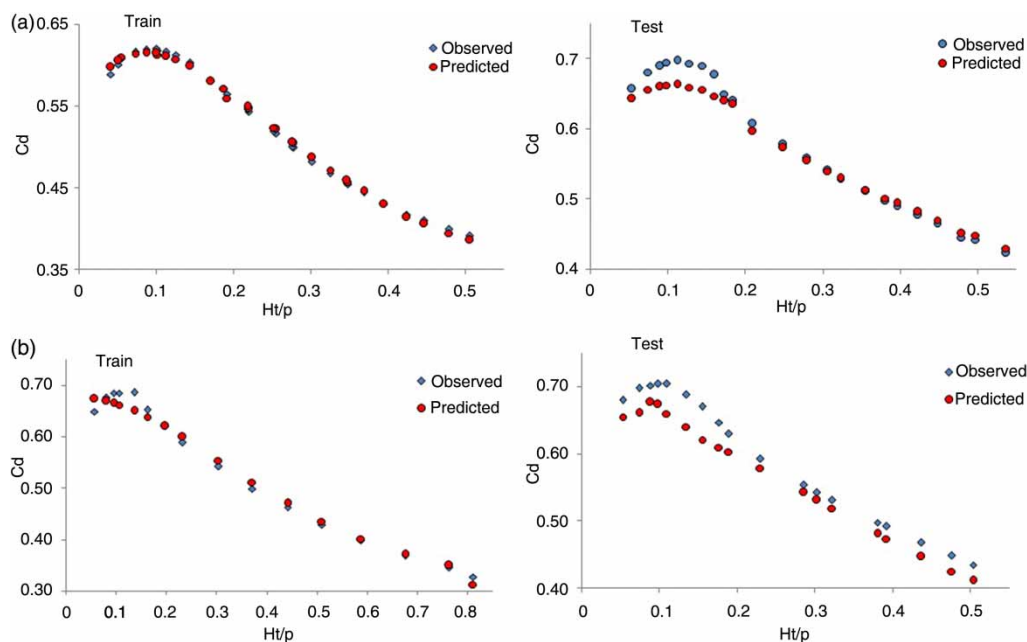
Figure 6 │ C_d vs. H_T/P variations for: (a) normal labyrinth weir (input configuration 10), (b) inverted labyrinth weir (input configuration 9).

would show the risk of overfitting (due to ignoring most of the support vectors), while its large values increase the complexity of the model (Han *et al.* 2007). A trial and error process was applied for all the input combinations to determine the optimum values of the SVM parameters.

Normal and inverted orientation labyrinth weirs in flume (NLW, ILW)

The dimensionless parameters evaluated in this section were: head water ratio (H_T/P), upstream Froude number (Fr), magnification ratio (L_c/W), sidewall angle (α), apex ratio (A/w) and cycle width ratio (w/p). To obtain the appropriate SVM model for determining the discharge coefficient of normal and inverted orientation labyrinth weirs, ten different input combinations were developed (see Table 3). Table 5 sums up the statistical indices of different SVM models. From the table it is clear that the input combination 10 (NLW 10) comprising the H_T/P, L_c/W, A/w and Fr dimensionless parameters as input variables, showed the most accurate results for the normal orientation labyrinth weir, with the lowest *RMSE* (0.007 and 0.007), and the highest *NS* (0.991 and 0.988) and R^2 (0.992 and 0.990) values for the train and test stages,

respectively. Attending to the inverted orientation labyrinth weir, the SVM9 model (fed with ILW 9 input configuration) comprising the H_T/P, α, L_c/W, A/w, w/p and Fr dimensionless parameters as input vectors gives the most accurate results with the lowest *RMSE* (0.015 and 0.025), and the highest *NS* (0.981 and 0.954) and R^2 (0.982 and 0.981) values, for the train and test stages, respectively. Analyzing the results shows that the input combinations which include the Fr number as an input parameter produce better results for both the normal and inverted orientation labyrinth weirs. Figure 5 represents the observed vs. simulated C_d values for optimum SVM models of the normal and inverted labyrinth weirs in both the train and test stages. From the figure it is seen that there is a good agreement between the observed and SVM-based simulated C_d values for both the studied weirs in the train and test stages. The discharge coefficient, C_d, is also presented as a function of H_T/P for the best model of normal and inverted orientation labyrinth weirs in Figure 6. From the figure it can be observed that for the lowest H_T/P values (peak C_d observations), the discrepancy between the observed and simulated C_d values presents higher magnitudes when compared to the higher H_T/P values. Analysis of the differences between the observed and simulated C_d
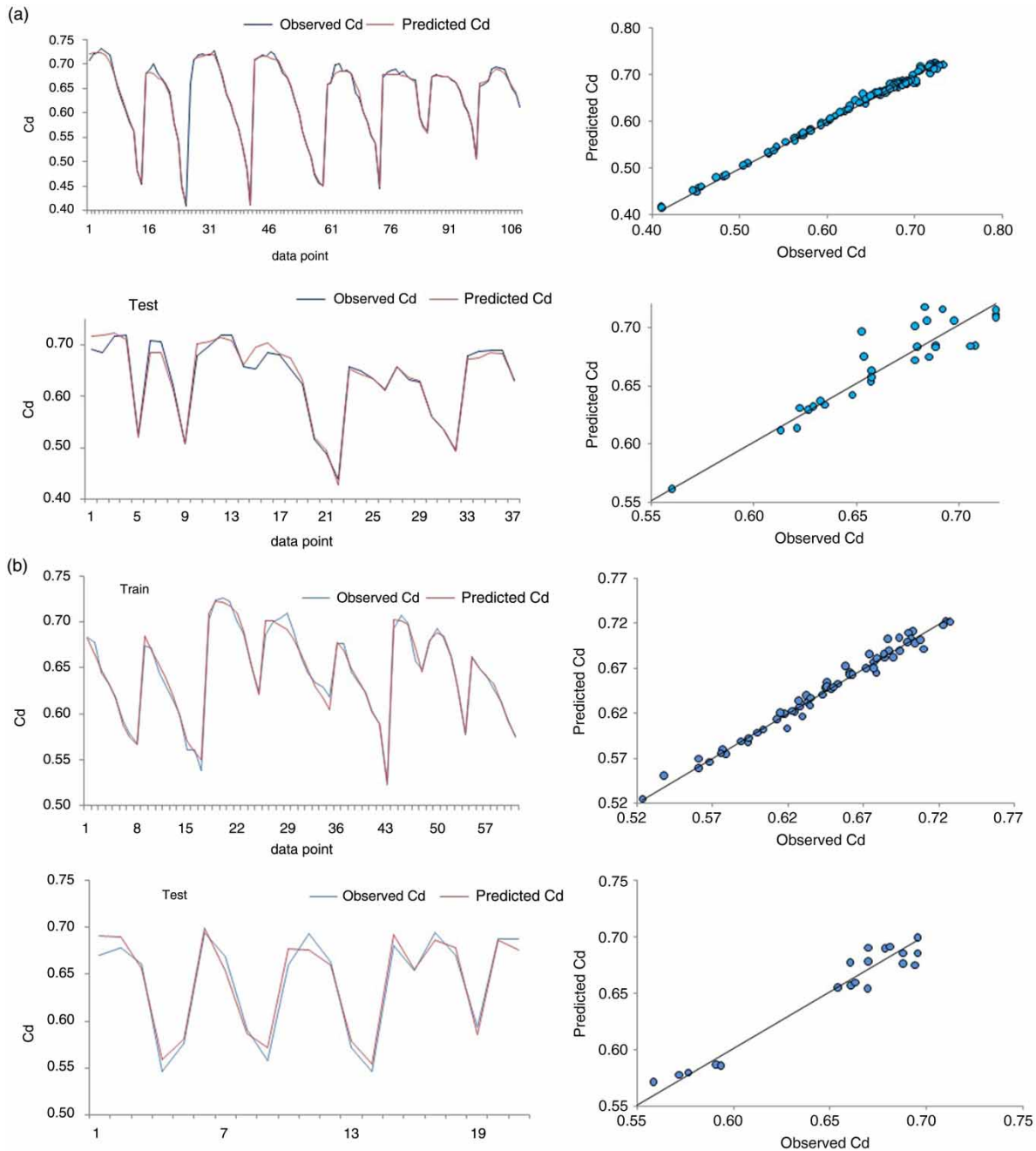
Figure 7 │ Observed vs. predicted discharge coefficient for the best models (model 7) of arced labyrinth weirs: (a) without nappe breakers, and (b) with nappe breakers.

values in these points (not presented here) shows that there is good agreement between observed and simulated values at large values of H_T/P, while, large differences can be detected for $H_T/P < 0.2$ (approximately 4%). This may be attributed to variation of the observed discharge coefficient around peak point values.

Arced labyrinth weirs with and without nappe breakers (ALW, ALWB)

Input parameters used to feed the SVM models in this part were the head water ratio (H_T/P), angle ratio (α/θ), number of cycles (N), magnification ratio (L_c/W), and relative
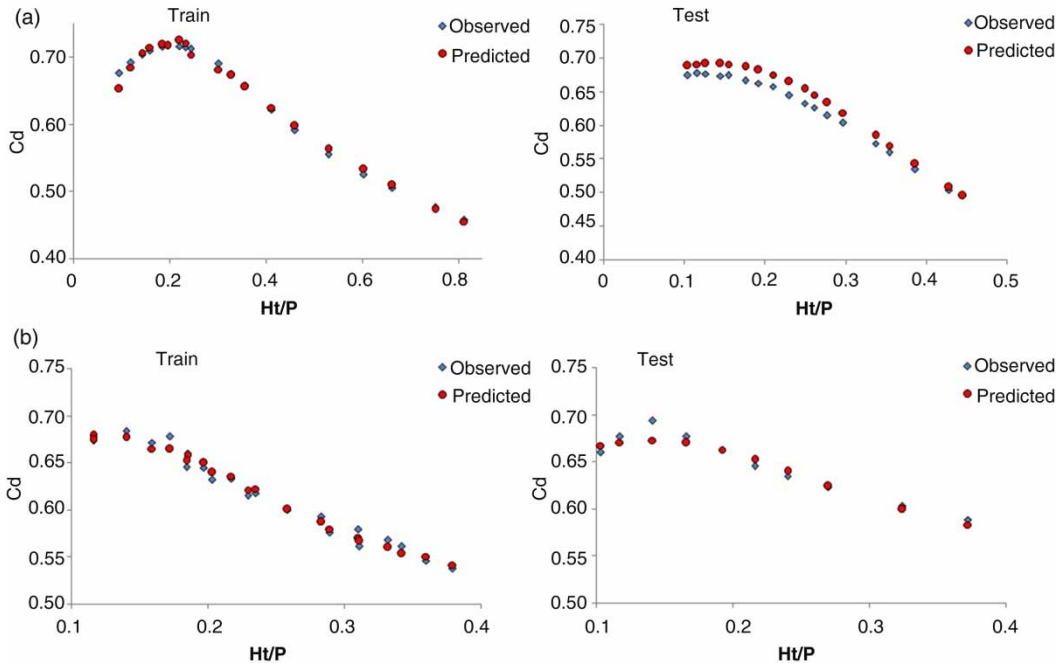
Figure 8 │ C_d vs. H_T/P variations for arced labyrinth weirs (model 7): (a) without nappe breakers, (b) with nappe breakers.

thickness ratio (P/t_w). To evaluate the best combination of these input parameters for determining the discharge coefficient of arced labyrinth weirs, eight input combinations were defined, as have been given in Table 3. The corresponding statistical indices are listed in Table 5. From the table it is clear that model 7, which includes the H_T/P, α/θ and L_c/W as input parameters, presents the lowest *RMSE* (0.013) and highest *NS* (0.967) and R^2 (0.970) values for arced labyrinth weirs without nappe breakers, and also shows the lowest *RMSE* (0.010) and highest *NS* (0.958) and R^2 (0.960) values for arced labyrinth weirs with nappe breakers in the testing stage. Figure 7 illustrates the observed vs. simulated values of C_d for train and test stages. The values of H_T/P were plotted against the observed and simulated C_d, in Figure 8. As can be seen from

Figures 7 and 8, the discharge coefficients from the SVM technique are in good agreement with the experimental data. Maximum error is observed at the low values of H_T/P, while the error decreased at higher H_T/P values. From Figure 7 it is seen that the SVM is trapped in overestimation in prediction of the discharge coefficient of arced labyrinth weirs without nappe breakers in the testing stage, and the mean error of the SVM model is between 1% and 3%. Table 6 summarizes the optimum SVM-based models of the studied cases.

DATA PROCESSING

Re-construction of input matrix

Figures 6 and 8 show that there is good agreement between the simulated and observed discharge coefficients at high values of H_T/P, while the largest differences are detected for $H_T/P < 0.2$. On the other hand, owing to the fact that the labyrinth weirs are employed for conveying the flow from upstream to downstream at the maximum discharge events, the data corresponding to $H_T/P < 0.2$ were eliminated from the input-target matrix, then the SVM model was re-established. The results showed that by eliminating these

**Table 6** │ Best models, evaluation criteria and effective parameters

Kind of labyrinth	Best model	Effective parameters	R^2	DC	RMSE
NLW	Model 10	(H_T/P-L_c/W-A/w-Fr)	0.990	0.9881	0.0077
ILW	Model 9	(H_T/P-α-L_c/W-A/w-w/p-Fr)	0.981	0.9536	0.0258
ALW	Model 7	(H_T/P-L_c/W-α/θ)	0.970	0.9671	0.0130
ALWB	Model 7	(H_T/P-L_c/W-α/θ)	0.960	0.9589	0.0104

Table 7 │ Data processing results

a) Analysis result of models re-construction

| Types of labyrinth weirs | Evaluation criteria in testing stage | | | | | |
| | Whole data | | | Re-constructed data | | |
	R^2	DC	RMSE	R^2	DC	RMSE
NLW (3)	0.889	0.872	0.026	**0.954**	**0.941**	**0.015**
INW (3)	0.878	0.878	0.035	**0.940**	**0.933**	**0.019**
ALW (3)	0.944	0.935	0 .015	**0.976**	**0.971**	**0.010**
ALWB (3)	0.833	0.813	0.037	**0.912**	**0.898**	**0.023**

b) Analysis results of data merging

| Types of labyrinth weirs | Evaluation criteria in testing stage | | | | | |
| | Separate data | | | Merged data | | |
	R^2	DC	RMSE	R^2	DC	RMSE
NLW (10)	0.990	0.988	0.007	–	–	–
INW (9)	0.981	0.953	0.025	–	–	–
Combination (NLW & INW) (10)	–	–	–	**0.915**	**0.901**	**0.045**
ALW (7)	0.970	0.971	0.013	–	–	–
ALWB (7)	0.960	0.958	0.010	–	–	–
Combination (ALW & ALWB) (7)	–	–	–	**0.871**	**0.866**	**0.052**
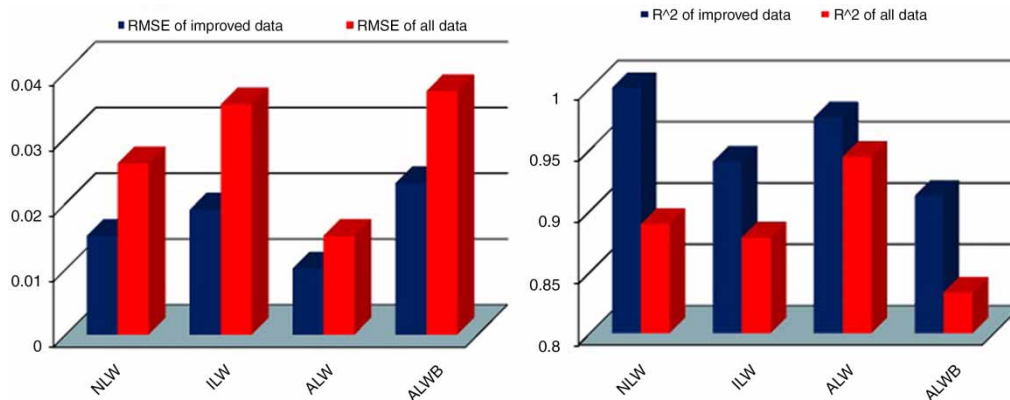
Figure 9 │ Comparison of original and re-constructed SVM statistics.

data, SVM model accuracies were improved for all labyrinth weirs models to a great extent (Table 7(a) and Figure 9).

Merging data

In this part of the study, all canal data (227 patterns) (data sets of normal and inverted orientation labyrinth weirs) as well as all reservoir data (300 patterns) (arced labyrinth weirs with and without nappe breakers), were combined separately, and the SVM models were established using the pooled data for each category using the previously applied input combinations. The results of the testing stage are presented in Table 7(b) and Figure 10. As can be seen from the table, model 10 shows the most accurate results in canal
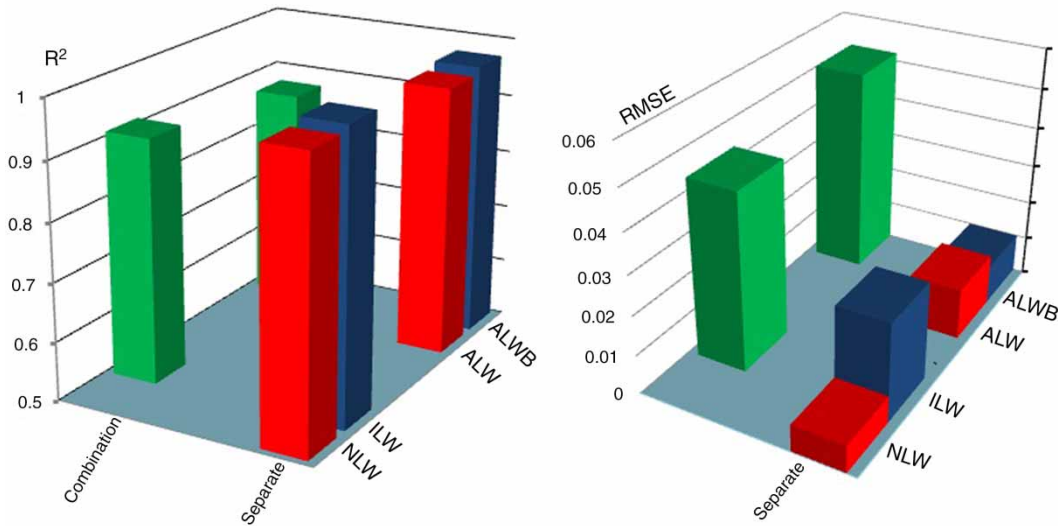
Figure 10 │ Comparing the results of combination data and separated data (testing stage).

Table 8 │ Result of sensitivity analysis

			Statistical indicators		
The best SVM models	**Input combinations**	**Eliminated variable**	R^2	**DC**	**RMSE**
NLW 10	$H_T/P, L_c/W, A/w, Fr$	–	0.990	0.988	0.007
	$H_T/P, L_c/W, A/w$	Fr	**0.921**	**0.910**	**0.020**
	$L_c/W, A/w, Fr$	H_T/P	0.931	0.913	0.019
	$H_T/P, A/w, Fr$	L_c/W	0.964	0.958	0.016
	$H_T/P, L_c/W, Fr$	A/w	0.977	0.961	0.015
The best SVM model	**Input combination**	**Eliminated variable**	R^2	**DC**	**RMSE**
ILW 9	$H_T/P, \alpha, L_c/W, A/w, w/p, Fr$	–	0.981	0.954	0.025
	$H_T/P, \alpha, L_c/W, A/w, w/p$	Fr	**0.915**	**0.913**	**0.029**
	$\alpha, L_c/W, A/w, w/p, Fr$	H_T/P	0.933	0.915	0.029
	$H_T/P, L_c/W, A/w, w/p, Fr$	α	0.965	0.960	0.026
	$H_T/P, \alpha, A/w, w/p, Fr$	L_c/W	0.950	0.942	0.027
	$H_T/P, \alpha, L_c/W, A/w, Fr$	A/w	0.966	0.960	0.026
	$H_T/P, \alpha, L_c/W, A/w, Fr$	w/P	0.964	0.958	0.026
The best SVM model	**Input combination**	**Eliminated variable**	R^2	**DC**	**RMSE**
ALW 7	$H_T/P, L_c/W, \alpha/\theta$	–	0.970	0.967	0.013
	$L_c/W, \alpha/\theta$	H_T/P	**0.651**	**0.606**	**0.098**
	$H_T/P, \alpha/\theta$	L_c/W	0.952	0.943	0.016
	$H_T/P, L_c/W$	α/θ	0.942	0.929	0.017
The best SVM model	**Input combination**	**Eliminated variable**	R^2	**DC**	**RMSE**
ALWB 7	$H_T/P, L_c/W, \alpha/\theta$	–	0.960	0.958	0.010
	$L_c/W, \alpha/\theta$	H_T/P	**0.623**	**0.431**	**0.107**
	$H_T/P, \alpha/\theta$	L_c/W	0.915	0.913	0.033
	$H_T/P, L_c/W$	α/θ	0.831	0.511	0.040

simulations, while model 7 presents the highest accuracy in the reservoir simulations. The results show that in the case of data scarcity, pooling the available data might be a promising approach for determining the discharge coefficient.

SENSITIVITY ANALYSIS

Sensitivity tests have been conducted to determine the relative significance of each of the independent parameters on C_d. Consequently, one input parameter was eliminated each time and the SVM models were re-established and re-evaluated. The results of this analysis are given in Table 8. As can be seen from this table, Froude number (Fr) and head water ratio (H_T/P) are the most influential parameters on C_d in normal and inverted orientation labyrinth weirs, respectively. For arced labyrinth weirs with and without nappe breakers, respectively, head water ratio (H_T/P) and angle ratio (α/θ) have the most significant effect on discharge coefficient.

CONCLUSIONS

The purpose of the present research was to provide new insights and design information regarding the performance and operation of normal and inverted orientation and arced labyrinth weirs, using SVM-based approaches. A total of 527 laboratory data and three statistical indices were used to evaluate the models' accuracies. To obtain the appropriate SVM model for determining the discharge coefficient of normal and inverted orientation labyrinth weirs, ten different input configurations were introduced to the SVM-based models. In the case of the arced labyrinth weirs, eight different input configurations were introduced. The obtained results revealed that there were good agreements between C_d values obtained by the SVM-based models and the observed C_d values for all labyrinth weirs, with the largest discrepancy of 4%, which was observed at low values of H_T/P. The results of the sensitivity analysis showed that the Froude number (Fr) and head water ratio (H_T/P) parameters are the most effective variables on the labyrinth weirs in canals, while the head water ratio and

angle ratio (α/θ) are the most effective variables on arced labyrinth weirs in reservoir, for determining the discharge coefficient. It should, however, be noted that the efficiency of the SVM-based models is data sensitive, so further studies using more laboratory or field data should be carried out to strengthen the outcomes of the present study.

REFERENCES

ASCE 2000 *Hydraulic Modeling: Concepts and Practice, Manual 97*, ASCE, Reston, VA.

Azamathulla, H. Md. & Chen Wu, F. 2011 Support vector machine approach for longitudinal dispersion coefficients in natural streams. *Applied Soft Computing* **11** (2), 2902–2905.

Azamathulla, H. Md., Haghiabi, A. H. & Parsaie, A. 2016 Prediction of side weir discharge coefficient by support vector machine technique. *Water Science & Technology: Water Supply* **16** (4), 1002–1016. doi:10.2166/ws.2016.014.

Bagheri, S., Kabiri-Samani, A. R. & Heidarpour, H. 2014 Discharge coefficient of rectangular sharp-crested side weirs, part II: Domínguez's method. *Flow Measurement and Instrumentation* **35**, 116–121.

Baylar, A., Hanbay, D. & Batan, M. 2009 Application of least square support vector machines in the prediction of aeration performance of plunging over-fall jets from weirs. *Expert Systems with Applications* **36** (4), 8368–8374.

Christensen, N. A. 2012 *Flow Characteristics of Arced Labyrinth Weirs*. MSc Thesis, Utah State University, Logan, UT.

Cimen, M. 2008 Estimation of daily suspended sediments using support vector machines. *Hydrological Sciences Journal* **53** (3), 656–666.

Cortes, C. & Vapnik, V. N. 1995 Support-vector networks. *Machine Learning* **20** (3), 273–297.

Crookston, B. M. 2010 *Labyrinth Weirs*. PhD Dissertation, Utah State University, Logan, UT.

Crookston, B. M. & Tullis, B. 2010 Hydraulic performance weirs. In: *Proc. of the Int. Junior Researcher and Engineer Workshop on Hydraulic Structures (IJREWHS '10)*. Edinburgh, UK.

Crookston, B. M. & Tullis, B. 2012 Labyrinth weirs: nappe interference and local submergence. *Journal of Irrigation and Drainage Engineering* **138**, 757–765.

Gentilini, B. 1940 Stramazzi con cresta a planta obliqua e a zig-zag (Weirs with planta oblique crest and zig-zag). Memorie e Studi dell Instituto di Idraulica e Construzioni Idraulic hedel Regil Politecnico di Milano, No. 48 (in Italian).

Goel, A. 2013 Modeling aeration of sharp crested weirs by using support vector machines. *International Journal of Computer and Information Engineering* **7** (12), 2620–2625.

Gorgij, A. D., Kisi, O. & Moghaddam, A. A. 2017 Groundwater budget forecasting, using hybrid wavelet-ANN-GP modelling:

a case study of Azarshahr Plain, East Azerbaijan, Iran. *Hydrology Research* **48** (2), 455–467. doi:10.2166/nh. 2016.202.

Han, D., Chan, L. & Zhu, N. 2007 Flood forecasting using support vector machines. *Journal of Hydroinformatics* **9** (4), 267–276.

Hanbay, D., Baylar, A. & Batan, M. 2009 Prediction of aeration efficiency on stepped cascades by using least square support vector machines. *Expert Systems with Applications* **36** (3), 4248–4252.

Hay, N. & Taylor, G. 1970 Performance and design of labyrinth weirs. *Journal of Hydraulic Engineering* **96** (11), 2337–2357.

Henderson, F. M. 1966 *Open Channel Flow*. Macmillan, New York, USA.

Kocahan, H. & Taylor, G. 2002 *Rehabilitation of Black Rock Dam 'Seepage & Inadequate Spillway'*. Hydroplus, Inc., Arlington, VA.

Li, X., Sha, J. & Wang, Z. L. 2017 A comparative study of multiple linear regression, artificial neural network and support vector machine for the prediction of dissolved oxygen. *Hydrology Research* **48** (5), 1214–1225. doi:10.2166/nh.2016.149.

Lux, F. & Hinchcliff, D. 1985 Design and construction of labyrinth spillways. In: *15th Congress ICOLD, Vol. IV, Q59-R15*, Lausanne, Switzerland, pp. 249–274.

Mohamed, K. & Oliver, B. 2005 Development of a discharge equation for side weirs using artificial neural networks. *Journal of Hydroinformatics* **7** (1), 31–39.

Parsaie, A. & Haghiabi, A. H. 2014 Assessment of some famous empirical equation and artificial intelligent model (MLP, ANFIS) to predicting the side weir discharge coefficient. *Journal of Applied Research in Water and Wastewater* **2**, 75–79.

Parsaie, A., Yonesi, H. A. & Najafian, S. H. 2015 Predictive modeling of discharge in compound open channel by support

vector machine technique. *Modeling Earth Systems and Environment*. doi:10.1007/s40808-015-0002-9.

Roushangar, K. & Koosheh, A. 2015 Evaluation of GA-SVR method for modeling bed load transport in gravel-bed rivers. *Journal of Hydrology* **527**, 1142–1152.

Roushangar, K., Akhgar, S., Salmasi, F. & Shiri, J. 2014a Modeling energy dissipation over stepped spillways using machine learning approaches. *Journal of Hydrology* **508**, 254–265.

Roushangar, K., Vojoudi, F. & Shiri, J. 2014b Modeling river total bed material load discharge using artificial intelligence approaches (based on conceptual inputs). *Journal of Hydrology* **514**, 114–122.

Seamons, T. R. 2014 *LabyrinthWeir: A Look into Geometric Variation and its Effect on Efficiency and Design Method Predictions*. MSc Thesis, Utah State University, Logan, UT.

Singh, K. K., Pal, M., Ojha, C. S. P. & Singh, V. P. 2008 Estimation of removal efficiency for settling basins using neural networks and support vector machines. *Journal of Hydrologic Engineering* **13** (3), DOI: http://dx.doi.org/10.1061/(ASCE)1084-0699 (2008).

Sivapragasam, C. & Muttil, N. 2005 Discharge rating curve extension: a new approach. *Water Resources Management* **19** (5), 505–520.

Taylor, G. 1968 *The Performance of Labyrinth Weirs*. PhD Thesis, University of Nottingham, Nottingham, UK.

Vapnik, V. 1995 *The Nature of Statistical Learning Theory, Data Mining and Knowledge Discovery*, 1–47. Springer-Verlag New York, Inc., New York.

Vapnik, V. 1998 *Statistical Learning Theory*. Wiley, New York.

Yin, Z. L., Wen, X. L., Feng, Q., He, Z. B., Zou, S. B. & Yang, L. S. 2017 Integrating genetic algorithm and support vector machine for modeling daily reference evapotranspiration in a semi-arid mountain area. *Hydrology Research* **48** (5), 1177–1191. doi:10.2166/nh.2016.205.